NOTICE CONCERNING COPYRIGHT RESTRICTIONS

Preliminary Investigation of Scale Formation and Fluid Chemistry at the Dixie Valley Geothermal Field, Nevada

Carol J. Bruton[1], Dale Counce[2], Deborah Bergfeld[2], Fraser Goff[2],
Stuart D. Johnson[3], Joseph N. Moore[4] and Gregory Nimz[1]

[1]Lawrence Livermore National Laboratory
[2]Los Alamos National Laboratory
[3]Oxbow Power Services, Inc.
[4]Energy & Geoscience Institute

ABSTRACT

The chemistry of geothermal, production, and injection fluids at the Dixie Valley Geothermal Field, Nevada, was characterized to address an ongoing scaling problem and to evaluate the effects of reinjection into the reservoir. Fluids generally followed mixing-dilution trends. Recharge to the Dixie Valley system apparently originates from local sources. The low-pressure brine and injection waters were saturated with respect to amorphous silica, which correlates with the ongoing scaling problem. Local shallow groundwater contains about 15% geothermal brine mixed with regional recharge. The elevated Ca, Mg, and HCO_3 content of this water suggests that carbonate precipitation may occur if shallow groundwater is reinjected. Downhole reservoir fluids are close to equilibrium with the latest vein mineral assemblage of wairakite-epidote-quartz-calcite. Reinjection of spent geothermal brine is predicted to affect the region near the wellbore differently than it does the region farther away.

Introduction

The Dixie Valley geothermal system supports a 62 MWe double-flash power plant, which became operational in 1988 after 12 years of exploration and development. The power plant and well field, owned and operated by Oxbow Geothermal Corp., have experienced some scaling problems. Scaling occurs on the downstream side of the power plant in flow lines to injectors and in the injectors themselves. Periodic cleaning is required. Oxbow is currently reinjecting spent geothermal brine into wells at the margin of the production zone, but is considering injecting a mixture of spent brine and local groundwater into the reservoir to maintain reservoir pressure.

Oxbow conducted several on-site tests of scale formation under conditions that are being considered for additional power generation through bottoming cycle low-pressure flash, and for mixing fluid flow streams to supplement reinjection with local shallow groundwaters. Oxbow operated a test skid incorporating 2.5- and 1.25-cm test spools at flow rates and residence times simulating plant and field conditions. Tests included Dixie Valley brines, which had been flashed in three stages down to a temperature of 88°C. In a separate test, low-pressure brine, steam condensate, and groundwater were mixed in a flow ratio of 6.5 gpm:1 gpm:2 gpm. Saturated low-pressure brines showed fairly uniform scaling rates for up to 1 hour residence times. Mixed flow streams produced more massive scale and accelerated scaling rates. Given the scaling problems and the planned operations at Dixie Valley, the following questions must be addressed:

- What is the source and composition of the scale that forms in the injection lines, and how can it be controlled?

- Will scale form if reinjection is supplemented with local shallow groundwater to maintain reservoir pressure? If so, how can it be controlled? Alternately, can waters be mixed in a way that limits scale formation, or should injection wells be dedicated to specific water sources?

- Will reinjection damage the reservoir over time?

A team from Los Alamos National Laboratory, Lawrence Livermore National Laboratory, and Energy & Geoscience Institute was assembled at the request of Oxbow Geothermal to help address these issues. In this paper, we discuss some preliminary results, including the chemical analyses of test skid scales, the characterization of fluid chemistry in the Dixie Val-

Table 1. Chemical composition of test bed scales

Component	Inlet	"Aged"	Exit
Major components (in wt%)			
SiO$_2$	62.10	61.56	60.52
Al$_2$O$_3$	7.47	6.60	3.84
Fe$_2$O$_3$	4.64	3.29	5.82
MnO	0.172	0.197	0.091
MgO	2.88	4.75	10.82
CaO	4.07	3.50	3.64
Na$_2$O	1.19	1.06	1.08
K$_2$O	1.53	1.38	1.02
P$_2$O$_5$	0.035	0.031	0.033
Cl	0.113	0.058	0.121
F	0.033	0.067	0.183
S	0.136	0.130	0.109
Total organic carbon	0.272	0.172	0.180
Total inorganic carbon	0.083	0.065	0.282
Selected minor components (in ppm)			
As	181	185	172
Cu	101	77	50
Li	18.5	18.3	170
Mo	4.0	6.1	<4
Ni	20.5	9.4	32.3
Sr	1180	2070	7

ley system, and the results of geochemical simulations of scale formation and fluid-mixing scenarios.

Geologic Setting

The Dixie Valley geothermal system is defined by fault and fracture permeability in a typical Basin and Range tectonic setting. The northeast-trending valley is about 120 km long by 20 km wide, bounded by the Stillwater Range on the west and the Clan Alpine Range to the east (Waibel, 1987; Honjas et al., 1997; Lutz et al., 1997). Geothermal fluids are produced from the subsurface extension of the normal Stillwater Fault and adjacent fractured rocks at depths of 2800 to 3050 m, but the fault zone architecture is complex (Caine et al., 1996). Convective heat flow in the geothermal system exceeds 300 mW/m^2. Conductive temperature gradients range from 100 to >200°C/km (Williams et al., 1997).

Paleozoic marine carbonates and siliciclastic rocks crop out in the Clan Alpine Range but have not been penetrated by Dixie Valley boreholes. Deeper geologic units penetrated by drilling are exposed in the Stillwater Range. Rocks consist of Triassic to Jurassic marine siltstones, shales, and volcaniclastic rocks overlain by the "Humboldt Lopolith" (Speed, 1976), a complex
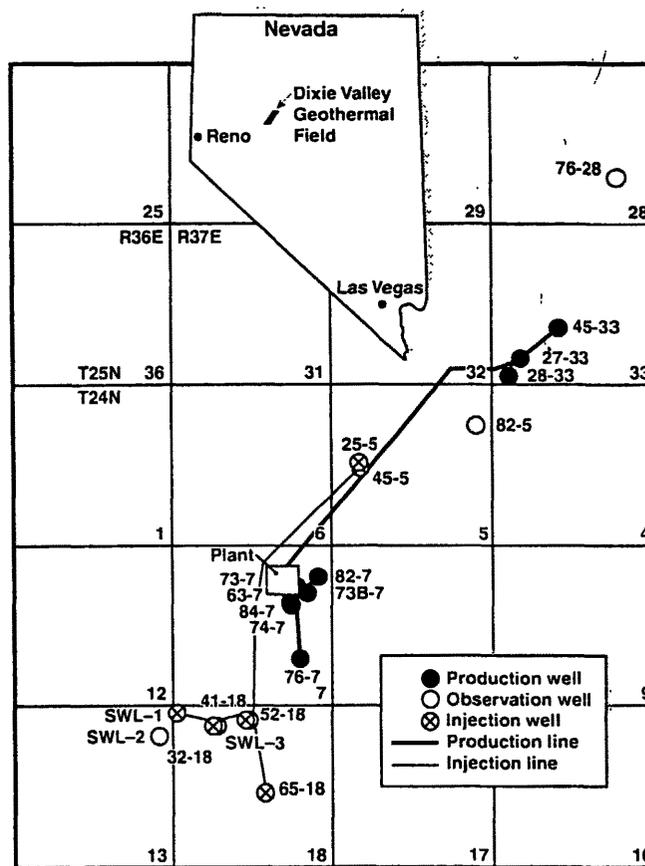
Figure 1. Map of the power plant and well field at the Dixie Valley Geothermal Field in Nevada.

of oceanic crustal rocks including gabbro, diorite, and basalt (Waibel, 1987; Lutz et al., 1997). The Triassic to Jurassic units have been imbricated into four similar stratigraphic packages by three thrust faults and were later intruded by Cretaceous granodiorite. Uplift and erosion exposed these older rocks by the mid-Tertiary, and the Miocene Table Mountain basalt rests on earlier rocks in both the range and the subsurface. Within Dixie Valley, the Miocene basalt is found at 1280 m below sea level and is overlain by a variety of late Tertiary basin-fill units. Extensive hydrothermal alteration from geothermal fluids has affected the rocks (Waibel, 1987; Lutz et al., 1997).

Chemical Analysis of Scale

X-ray diffraction (XRD) analysis of scales from the flashed brine and fluid-mixing tests revealed mainly the presence of amorphous silica. Minor and trace amounts of quartz, calcite, magnetite, goethite, and clays were identified. More detailed XRD analysis of the clay did not ascertain its nature.

Table 1 lists the chemical analyses of the scales that formed during the fluid-mixing test. Scales from the bottoming cycle low-pressure flash test and the injection line scale have not been analyzed as yet. According to S. D. Johnson, the inlet scale formed at the inlet to the first test bed. It was the youngest scale at the inlet and formed as an overgrowth on the "aged" sample, which also formed at the inlet. The "aged" sample was

Table 2. Fluid chemistry (in ppm except as noted). HCO_3 and CO_3 values were measured in the laboratory.

	DIXE 102-S	DIXE 102-W	DV96-1	DV96-2	DV96-3	DV96-4	DV96-5	DV96-6	DV96-7	DV96-8	DV96-9	DV 96-10
Temp. (°C)	—	—	34.2	41.8	110	107	107	—	163	163	166	166
Major elements												
SiO_2	—	—	74.3	1.67	644	601	618	629	4.6	599	599	4.19
Ca	—	7.92	61.6	1.3	8.74	8.38	9.55	8.68	0.15	8.53	8.03	0.22
Mg	—	0.04	32	0.12	0.027	0.023	0.014	0.009	<0.01	0.026	0.007	0.01
Sr	—	0.4	1.63	0.01	0.41	0.41	0.46	0.45	<0.01	0.43	0.37	<0.01
Na	2.74	462	143	0.65	493	470	506	506	1.05	474	407	0.96
K	—	71.8	15.4	0.11	73.4	72	74.6	75.2	1.03	69.5	64	1.33
Li	—	2.29	0.43	<0.01	2.61	2.5	2.52	2.57	<0.01	2.29	2.03	<0.01
HCO_3	34.9	0	305	7.5	0	0	0	0	51	32.8	18.2	42
CO_3	0	76.3	0	0	58	57.7	62.6	59.9	0	87.8	93.2	0
SO_4	3.35	225	194	26.4	228	213	224	226	1.26	201	196	1.96
Cl	3.1	495	105	0.42	519	518	549	556	0.26	524	438	0.13
F	0.07	17.6	0.78	0.01	17.8	15	16.2	16.1	0.03	13.4	15.5	0.01
Br	<0.02	0.49	0.12	<0.02	0.409	0.368	0.442	0.451	<0.02	0.441	0.321	<0.02
B	0.12	9.35	1.46	0.24	11.5	11.4	12.6	12.5	0.16	11.6	9.92	0.13
CO_3	0	76.3	0	0	58	57.7	62.6	59.9	0	87.8	93.2	0
Selected minor elements												
Al, total	—	1.41	0.2	0.14	1.27	1.21	1.39	1.35	<0.01	1.12	1.54	<0.01
Al^{+3}, 0.2μ [a]	—	—	0.0026	0.0096	0.025	0.0079	0.0004	0.0004	—	0.05	0.101	—
Al^{+3}, 0.45μ [a]	—	—	—	0.0106	0.011	0.0087	0.0004	0.0014	—	0.059	0.0088	—
As	—	0.46	0.052	0.0024	0.74	0.86	0.82	1.44	0.0037	0.51	0.47	0.0061
Fe	0.11	0.02	1.18	0.06	0.05	0.08	<0.01	0.02	1.02	0.02	<0.01	0.25
NH_4	11.4	1.46	0.17	26.3	1.02	2.9	0.95	0.91	14.6	2.13	1.84	12.7
NO_3	<0.02	<0.05	0.09	43.5	0.15	4.01	0.08	0.11	<0.02	0.19	<0.04	<0.02
Sr	—	0.4	1.63	0.01	0.41	0.41	0.46	0.45	<0.01	0.43	0.37	<0.01

a. 0.2μ and 0.45μ indicate the filter size used.

reddish-brown in color and very porous; the younger inlet scale is lighter in color and more dendritic. The exit scale formed on a dispersion plate at the exit to the test bed and is granular in appearance.

Chemical Analyses of Power Plant Fluids

Fluids were collected in October 1996 from the Dixie Valley power plant at the following locations (see also Figure 1):

1. Water well drilled to supply water for "domestic" use within the plant (DV96-1).

2. Condenser water at plant (DV96-2).

3. Low-pressure brine at plant (DV96-3).

4. North injection well Dixie Federal (D.F.) 25-5, injects mixture of low-pressure brine and condensate (DV96-4).

5. South injection well Lamb-1, injects low-pressure brine (DV96-5).

6. South injection well D.F. 65-18, injects low-pressure brine (DV96-6).

7. Production well D.F. 76-7, condensate at steam side of separator (DV96-7).

8. Production well D.F. 76-7, brine on brine side of separator (DV96-8).

9. 101 separator brine, combination of production from three wells (DV96-9).

10. 101 separator steam condensate, combination of production from three wells (DV96-10).

Chemical analyses of these fluids are listed in Table 2, and gas analyses in Table 3. Both were obtained with a combination of field and laboratory measurements according to methods of Trujillo et al. (1987). Samples were filtered to 0.45 and 0.2 μm. The Al3^{3+} was extracted following the method of Barnes (1975). Although measured values of CO_3 are reported, it is likely that components such as boron, silica, and ammonium ion may have interfered with this analysis. Calculations show that the presence of significant quantities of CO_3 is not consistent with the pH of the solutions.

The condensate and brine from well D.F. 76-7 are sourced from one production zone in the reservoir. The steam fraction in D.F. 76-7 was calculated to be about 0.18 to 0.189; extremely good agreement was found between enthalpy balance calculations and relative mass flows of brine and steam.

Variation in concentrations of As, B, Br, and Li with respect to Cl for production, domestic, and injection fluids defines

mixing-dilution lines (Figure 2). Some samples do not seem to follow the mixing-dilution line (e.g., As). Additional sampling is required to verify these measurements.

The mixing-dilution lines suggest that the domestic water contains a mixture of meteoric recharge and up to 25% of reservoir fluid, depending on the salinity of the recharge. This helps to explain the high HCO_3 SO_4, and Ca contents of the water. The north injection fluids are less concentrated than the south injection fluids because the former contains about 5% condenser water as a dilutant. However, the south injection fluids are more concentrated than the low-pressure brine, which indicates that the low-pressure brine sample is not representative of the fluid leaving the power plant. No cause for the discrepancy has been identified. Steam loss causes the shift along the mixing-dilution line between each reservoir fluid and its separator brine.

Isotope Geochemistry

Isotopic compositions of Dixie Valley thermal, non-thermal, and injection fluids are listed in Table 4 and plotted in Figure 3. Tritium values of production fluids are less than 0.12
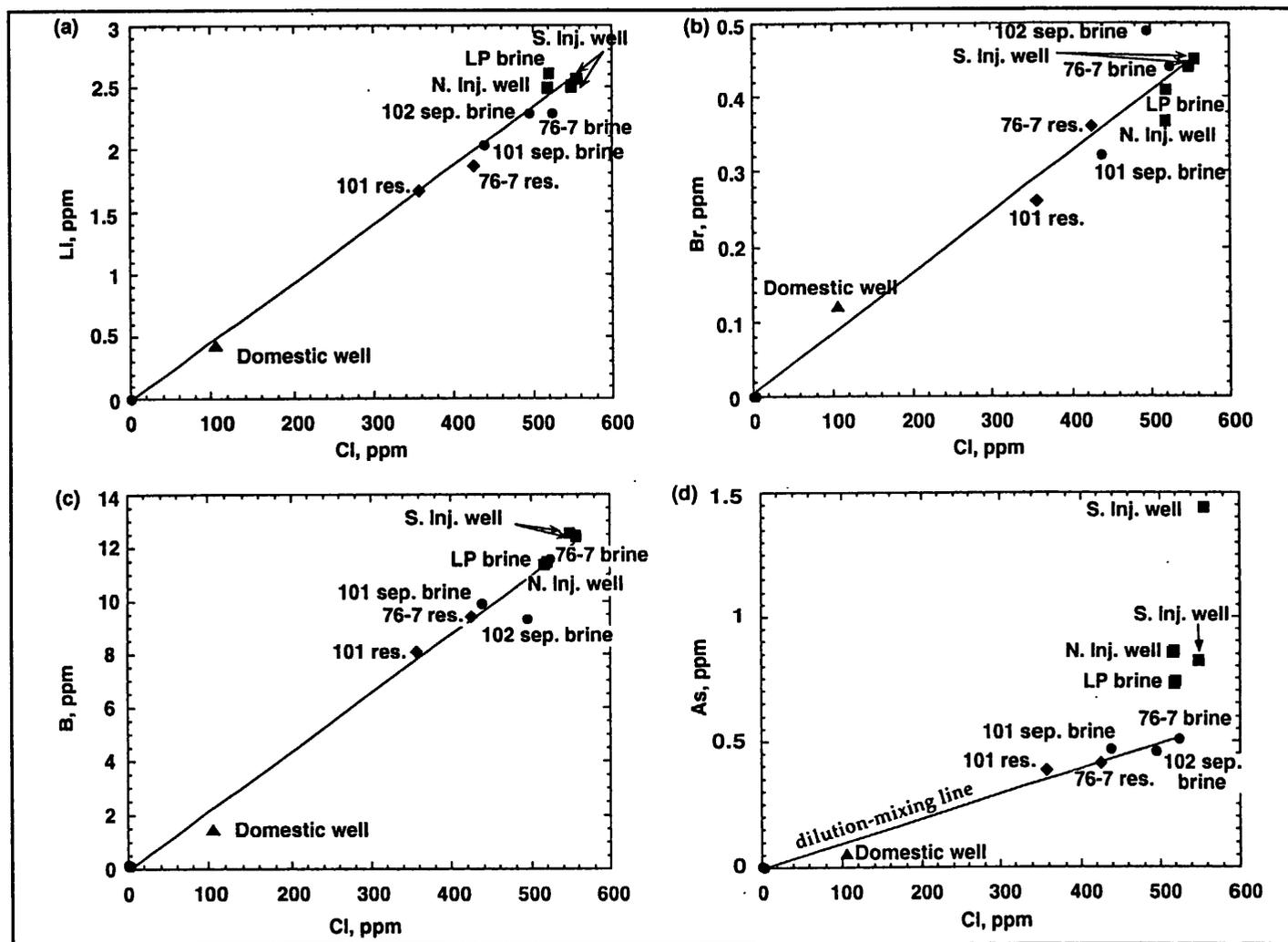
Figure 2. (a) Li, (b) Br, (c) B, and (d) As concentrations as a function of Cl concentration in Dixie Valley waters. Symbols: ● = separator brines and steam condensates, ■ = injection wells and low-pressure brine, ◆ = calculated reservoir, and ▲= domestic water.

T.U., indicating that the fluids are relatively old (>75 years). Dixie geothermal brines show an oxygen isotope enrichment of 2 to 3‰ due to high-temperature rock-water interactions. The downhole composition of the reservoir fluids was calculated from the isotope values for brine and separated steam at separation temperature and pressure using methods described in Henley et al. (1984, p. 135). The values lie directly to the right of the isotopic composition of local groundwater (domestic), which suggests that recharge to the Dixie geothermal system occurs locally. This assertion must be checked by comparing compositions with those of other nearby meteoric fluids.

Condenser water shows extreme isotopic enrichment due to · evaporation in the cooling towers. Injection fluids (LP brine and Inj. wells) show slight isotope enrichments from loss of steam. The north injection well is a mixture of LP brine and a small amount of condenser fluid, as reflected in its isotopic composition. LP brine should have the same isotopic composition as the south injection wells if other fluids and steam are not added or lost. The isotopic differences may be analytical. However, the elemental chemistry of these fluids shows slight chemical differences as well.

The carbon isotope compositions of separated CO_2 are –4.5 to –5.3‰ (Table 4) and isotope values of downhole compositions are –5.3 to –5.0‰ (Henley et al., 1984). These values fall within the range of mantle values (–3 to –8‰). A noble gas investigation of separator fluids by Kennedy et al. (1996) indicated that <10% of reservoir He is mantle-derived (R/R_A of 0.70–0.76). Thus, carbon in the system may originate from carbonate and organic sources with isotopically enriched and depleted carbon, respectively.

The $^{36}Cl/Cl$ ratio was measured in four Dixie Valley waters within and proximal to the geothermal field (Table 4). Three samples (DV-3, -8, -9) were geothermal brines with $^{36}Cl/Cl$ ratios of about 50 x 10^{-15}. Two of these were production samples collected before the water enters the power plant, and one was collected just as the water leaves the plant and prior to reinjection. The uniformity of the $^{36}Cl/Cl$ values indicates that no significant amounts of chloride are added to the brines while within the power plant system. Therefore reinjection of the brine does not alter the natural $^{36}Cl/Cl$ ratio within the field.

The $^{36}Cl/Cl$ ratio of local groundwater (167 x 10^{-15}) was substantially higher than the brines, but lower than expected for regional precipitation (>320 x 10^{-15}; Bentley et al., 1986). This suggests that local shallow groundwaters are a mixture of regional recharge and deeper geothermal brines. Mixing calculations indicate that if the regional recharge has a typical chloride concentration of 50 ppm and a $^{36}Cl/Cl$ of 320 x 10^{-15}, then about 12% of the sampled groundwater is geothermal brine.

Geochemical Characterization of Fluid Chemistry

The sampled fluids were characterized with the Geochemist's Workbench software package (Bethke, 1996). Thermodynamic data were taken from version COM.V8.R5 of the GEMBOCHS database (Johnson and Lundeen, 1997). Fluid pressures were assumed to correspond to the liquid/vapor saturation curve for pure H_2O. Selected analyses are described below.

Domestic water. Domestic water is slightly supersaturated with respect to calcite. The SiO_2 concentration is similar to that controlled by the silica polymorph β-cristobalite, but may be controlled instead by near-surface weathering processes or by incorporation of geothermal brine. Various clays, especially

Table 3. Gas analyses (in mol % dry gas except where noted). No measurable concentraction of CO, Hbr, or HC1 were detected.

	DIXE102G	DV96-7a	DV96-7b	DV96-7c	DV96-10a	DV96-10b
				Sample No.		
Temperature (°C)	—	163	163	163	166	166
H_2O collected (mol)	7.15	7.52	6.7	5.39	4.78	5.71
Total dry gas (mol)	0.007	0.0124	0.0095	0.0109	0.0093	0.004
He	0	0.00584	0.00219	0.00307	0.00331	0.00226
H_2	0	0.01247	0.01396	0.01952	0.02904	0.01635
Ar	0.0022	0.0134	0.0173	0.0325	0.0252	0.0302
O_2	0.0364	0.03	0.0491	0.0228	0.034	0.0201
N_2	0.1592	0.8024	1.0109	1.2722	1.3178	0.7569
CH_4	0.00289	0.45889	0.56345	0.82252	0.41353	0.22523
CO_2	96.63	97.49	96.86	96.62	96.56	96.4
NH_3	0.908769	0.686633	0.829625	0.626418	0.618786	1.791516
H_2S	2.053	0.56	0.629	0.562	1.147	0.623
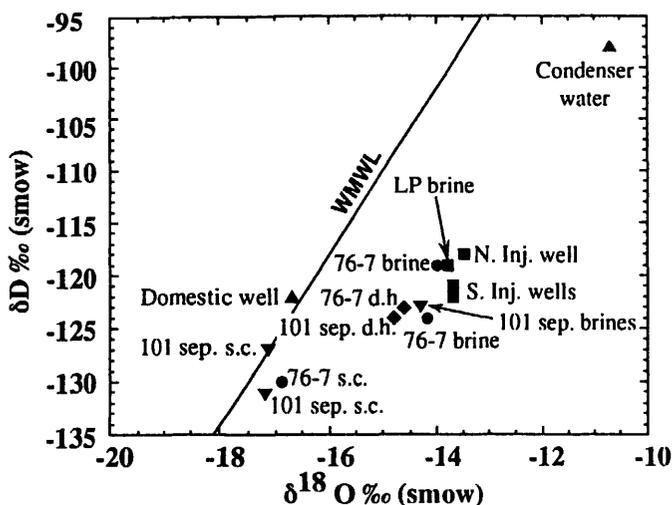
Figure 3. Plot of δD vs. δ¹⁸O for geothermal fluids from the Dixie Valley power plant. Smow = standard mean ocean water; WMWL = world meteoric water line.

Figure 4. Saturation, expressed in terms of logarithm of Q/K, of selected minerals versus temperature for reconstructed downhole water chemistry in well D.F. 76-7, calculated using 0.92 mg/kg total Al in solution.

Mg-bearing clays, are supersaturated with respect to the domestic water owing to its relatively high Mg concentrations.

The calculated fugacity of CO_2 equals about 0.01 bars, which exceeds atmospheric values. Hinkle (1995) reported CO_2 values far in excess of atmospheric values (up to 9.2%) in soil gases from the Dixie Valley production area. Near-surface biogenic processes can result in elevated CO_2 fugacities. However, elevated HCO_2 and SO_4 could also result from incorporation of geothermal fluids. As previously discussed, the mixing-dilution lines in Figure 2, the stable isotopes of water (Figure 3), and the $^{36}Cl/Cl$ isotopic ratios (Table 4) suggest that the domestic water is a mixture of meteoric recharge and geothermal brine.

Low-pressure brine and south injection waters at D.F. Lamb-1 and D.F. 65-18. The chemistries of these waters are similar except that their monomeric (Al^{3+}) content is higher in the low-pressure brine, which results in higher saturations with respect to aluminosilicates. However, they are almost exactly at saturation with amorphous silica, which suggests that during the flashing of the geothermal brines, silica has precipitated as necessary to maintain saturation with amorphous silica. At in-line temperatures (about 107°C), these waters have a pH of about 8.4. They are supersaturated with respect to calcite and Mg-bearing minerals, and undersaturated with respect to anhydrite.

Downhole reservoir fluid of production well D.F. 76-7. Geochemical modeling suggests that the pH of the reconstructed downhole fluid equals 6.8. The saturation state vs. temperature diagram[1] (Figure 4) shows that quartz is in equilibrium with the fluid at the reservoir temperature of 250°C, whereas calcite is slightly supersaturated. Calcite solubility is

highly dependent on the gas analysis used to reconstruct the downhole fluid. The stability of aluminosilicates is highly dependent on the Al concentration. K-feldspar and wairakite as well as quartz and calcite are close to equilibrium under reservoir conditions provided that the total measured Al concentration of 0.92 mg/kg is used (Figure 4). Clinozoisite, a compositional end-member of an epidote solid solution, is supersaturated. The predicted subsurface mineralogy agrees well with the Stage IV wairakite-epidote-quartz-calcite veins associated with present-day thermal fluids (Lutz et al., 1997).

Computer Simulations of Heating and Fluid Mixing

Conductive heating of domestic water. We simulated conductive heating of domestic water from 34°C, its collection temperature, to 250°C, the reservoir temperature, to study the
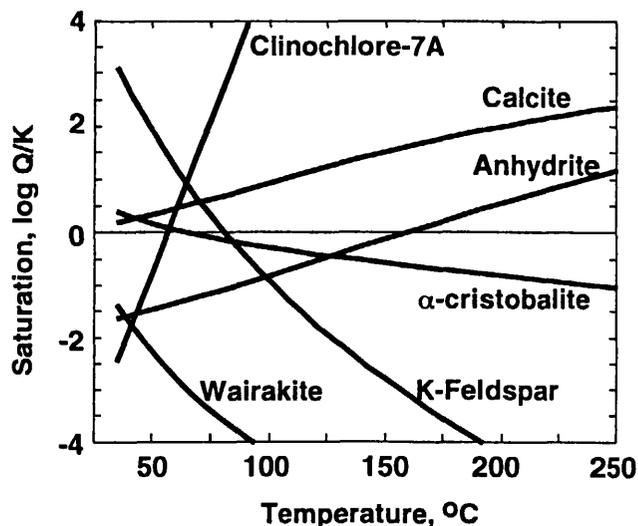
Figure 5. Saturation, expressed in terms of logarithm of Q/K, of selected minerals versus temperature during the conductive heating of domestic water.

[1]This diagram depicts the saturation state in terms of the logarithm of the ion activity product (Ω) divided by the equilibrium constant (K) of the hydrolysis reaction for each mineral. Zero denotes equilibrium, a positive value implies supersaturation, and a negative value indicates undersaturation. Saturation curves converge on zero at the downhole temperature.

Figure 6. Summary of chemical and mineralogic trends during gradual mixing of (a) injectate into reservoir fluid and (b) reservoir fluid into injectate. Abbreviations: Carb. = carbonates, satn. = saturation, SiO_2 = silica polymorphs, Mg-silicate = Mg-bearing silicates, Fsp = feldspar.

Temperature changes linearly as a function of mixing, whereas pH is controlled both by temperature and ongoing mineral precipitation/dissolution reactions. The simulations suggest that the stabilities of many minerals are affected mainly by changes in temperature during mixing, rather than variations in pH caused by mineral precipitation and dissolution. However, Mg-bearing silicates such as Mg-chlorite are more sensitive to the evolution of pH, and their precipitation and dissolution will likewise have a greater impact on pH.

Conclusions

The scale and fluids of the Dixie Valley system were chemically analyzed to evaluate the causes of scale formation and the potential effects of reinjection into the reservoir. Although research will continue to refine our knowledge of various reservoir and production processes, the data are sufficient to draw some conclusions about scale formation and reinjection. Geochemical modeling calculations indicate that the low-pressure brine and injection fluids are saturated with respect to amorphous silica, which is consistent with observed scale formation. Scale formed during on-site tests was composed of amorphous silica with minor to trace amounts of other minerals.

Simulations suggest that heating domestic water from a local shallow groundwater supply for reinjection purposes will favor the formation of carbonate, sulfate, and Mg-silicate scales, but will limit silica scale. The reinjection of low-pressure brine and its subsequent mixing with reservoir fluid can affect the region near the wellbore much differently than the region farther away. Mineral saturation states during mixing are largely controlled by changes in temperature. Some minerals, such as Mg-chlorite and other Mg-bearing silicates, are especially sensitive to changes in pH caused by changing temperature and ongoing mineral precipitation/dissolution reactions. Likewise, the precipitation and dissolution of Mg-bearing silicates will have a greater impact on pH.

potential consequences of its use in reinjection. Simulation results (Figure 5) suggest that carbonates, sulfates, and Mg-bearing silicates will tend to precipitate as domestic water is heated, but that non-Mg-silicates will become increasingly undersaturated as temperature increases, thereby lessening the potential for silica precipitation.

Mixing of injectate with reservoir waters. We simulated mixing of injectate with reservoir waters close to the wellbore and farther away. Near the wellbore, temperatures and salinities decrease as the cool injection water dilutes the reservoir fluid. Away from the wellbore, temperatures rise and salinities increase as the cool injection water is mixed with increasing proportions of hot reservoir fluid.

Modeling results from the mixing of injectate from well Lamb-1 with reservoir fluid (shown schematically in Figure 6) clearly show that completely different mineral reactions can occur depending on where mixing occurs and on which conceptual model is used for the mixing process. The main controls of the mineralogic trends appear to be temperature and pH.

Acknowledgments

References

Barnes, R.B., 1975. The determination of specific forms of aluminum in natural water: *Chem. Geology* 15, 177–191.

Bentley, H.W., Phillips, F.M., and Davis, S.N., 1986. Chlorine-36 in the terrestrial environment. In: *Handbook of Environmental Isotope Geochemistry*, Vol. 2, (P. Fritz and J.-Ch. Fontes, Eds.), p. 427–480.

Table 4. Isotopic values of Dixie Valley waters. Stable isotope values (in ‰) relative to SMOW and PDB.

Sample No.	Description	^{3}H, T.U.[a]	δD[b]	δ^{18}O[b]	δ^{13}C DIC[c]	δ^{13}C CO$_2$[c]	^{36}Cl/Cl[d] ($\times 10^{-15}$)	Run error ^{36}Cl/Cl ($\times 10^{-15}$)
DV96-1	Domestic well	0.11	−122	−16.7	−6.4		167	±4
DV96-2	Condenser water	0.35	−98	−10.7				
DV96-3	LP brine	0.17	−119	−13.8	−5.8		52	±2
DV96-4	North injection well	0.19	−118	−13.5				
DV96-5	South injection well		−122	−13.7				
DV96-6	South injection well		−121	−13.7				
DV96-7a	D.F. 76-7; condensate/gas		−130	−16.9		−5.3		
DV96-7b	D.F. 76-7		−130	−16.9				
DV96-7c	D.F. 76-7					−4.8		
DV96-8	D.F. 76-7 well	0.07			−8.0		45	±2
DV96-8a	D.F. 76-7 well		−124	−14.2				
DV96-8b	D.F. 76-7 well		−119	−14				
DV96-9	101 separator brine	0.12			−8.0		53	±2
DV96-9a	101 separator brine		−123	−14.3				
DV96-9b	101 separator brine		−123	−14.3				
DV96-10	101 sep. condensate/gas				−5.7			
DV96-10a	101 separator		−127	−17.1		−4.8		
DV96-10a	101 separator					−4.5		
DV96-10b	101 separator		−131	−17.2				

a. ^{3}H by H. Gröte Ostlund (University of Miami); error is ±10% of reported value. T.U. = tritium units.

b. δD, δ^{18}O by R.V. Krishnamurthy (Western Michigan University); errors are ±1‰ in δD and ±0.1‰ in δ^{18}O.

c. DIC = dissolved inorganic carbon. δ^{13}C by Geochron Laboratories, Cambridge, MA; error is ±0.2‰.

d. ^{36}Cl/Cl by G. Nimz (Lawrence Livermore National Laboratory).

Bethke, C.M., 1996. *Geochemical Reaction Modeling*: Oxford University Press, New York, 397 p.

Caine, J.S., Evans, J.P. and Forster, C.B., 1996. Fault zone architecture and permeability structure: *Geology* 24, p. 1025–1028.

Henley, R., Truesdell, A.H., Barton, P. and Whitney, J., 1984. *Reviews in Economic Geology*, Vol. 1: Fluid-Mineral Equilibria in Hydrothermal Systems: Soc. Econ. Geol., El Paso, TX, 267 p.

Hinkle, M., 1995. *Concentrations of N$_2$, O$_2$, CO$_2$, and He in Soil Gases Collected over and near the Dixie Valley Known Geothermal Resource Area, Northern Dixie Valley*, Nevada: U.S. Geological Survey Open-File Report 95-80.

Honjas, W., Pullammanappillil, S.K., Lettis, W.R., Plank, G.L., Louie, J.N. and Schweichert, R., 1997. Predicting subsurface structure within the Dixie Valley geothermal field, Dixie Valley, Nevada, using a non-linear optimization scheme: Geothermal Resources Council *Bulletin*, February, p. 45–52.

Johnson, J.W. and Lundeen, S.R., 1997. *GEMBOCHS Thermodynamic Data Files for Use with the EQ3/6 Software Package*: Lawrence Livermore National Laboratory Internal Report.

Kennedy, B., Benoit, D. and Truesdell, A., 1996. A preliminary survey of noble gases at Dixie Valley, Nevada: Geothermal Resources Council *Bulletin*, v. 20, p. 815–819.

Lutz, S.J., Moore, J.N. and Benoit, D., 1997. Geologic framework of Jurassic reservoir rocks in the Dixie Valley Geothermal Field, Nevada: Implications from hydrothermal alteration and stratigraphy: *Proceedings of the 22nd Workshop on Geothermal Reservoir Engineering*, Stanford University Report SGP-TR-155, Stanford, California, January 27–29, 8 p.

Speed, R.C., 1976. Geologic map of the Humboldt Lopolith: Geological Society of America Map Chart Series MC-14, 1:81050 scale, 1 sheet.

Trujillo, P., Counce, D., Grigsby, C., Goff, F. and Shevenell, L., 1987. *Chemical Analysis and Sampling Techniques for Geothermal Fluids and Gases at the Fenton Hill Laboratory*: Los Alamos National Laboratory Report LA-11006-MS, 84 p.

Waibel, A.F., 1987. An overview of the geology and secondary mineralogy of the high temperature geothermal system in Dixie Valley, Nevada: Geothermal Resources Council *Transactions*, v. 11, p. 479–486.

Williams, C.F., Sass, J.H., and Grubb, F.V., 1997. Thermal signature of subsurface fluid flow in the Dixie Valley geothermal field, Nevada: *Proceedings of the 22nd Workshop on Geothermal Reservoir Engineering*, Stanford University Report SGP-TR-155, Stanford, California, January 27–29, 8 p.